Fusion Engineering and Design 118 (2017) 81–97

Contents lists available at ScienceDirect

Fusion Engineering and Design

journal homepage: www.elsevier.com/locate/fusengdes

Design and implementation of wormlike creeping mobile robot for EAST remote maintenance system

Qiang Zhang[a,b], Ling Zhou[a], Zengfu Wang[a,b,*]

[a] Institute of Intelligent Machines, Chinese Academy of Sciences, Hefei, Anhui 230031, China
[b] Department of Automation, University of Science and Technology of China, Hefei, Anhui 230026, China

HIGHLIGHTS

- Wormlike creeping robot walking on the V-shaped circular slot in EAST fusion vessel.
- Mobile platform to carry equipments or assist manipulators for maintenance tasks.
- Chain structure design with n(n ≥ 2) creeping units each of which has three segments.
- Creeping gait planning to construct a multi-axis coordinating control scheme.
- Evaluation and verification of basic motion performance and mechanical properties.

ARTICLE INFO

Article history:
Received 18 May 2016
Received in revised form 4 March 2017
Accepted 13 March 2017
Available online 24 March 2017

Keywords:
EAST nuclear fusion vessel
Creeping walking mechanism
Mechanical property analysis
Gait planning
Movement performance test

ABSTRACT

Maintenance for nuclear fusion vessel is crucial, yet it faces great difficulty due to the complex internal physical and geometric conditions. Since the limitation on inherent strength, load, size, etc, a manipulator robot can only complete very limited tasks. Robotic arm systems for remote operation such as JET and MPD can carry certain tools to complete a variety of operating tasks, but it is difficult to achieve the system which is very complex. Therefore, if the inherent idea of using a single robot to complete the specified functions can change, it is possible to make the problems simpler and easier to solve by adding auxiliary robots working together with the robotic arm systems to complete the assigned tasks. Under the above background, based on the deeply analyzing and refining the functional requirements of the vessel operation robot, proceeding from the perspective of ability to move and carry a certain operating device, this paper presents a wormlike creeping mobile robot walking on the V-shaped circular slot inside a nuclear fusion vessel such as EAST (Experimental Advanced Superconducting Tokamak). We have designed and implemented the principle prototype of the robot which has chain structure with n (n ≥2) creeping units. Each creeping unit is of three-part structure, which consists of fore segment, mid segment and back segment connected by bidirectional universal joint. The fore and back segments stretch the paws to contact the surface of V-shaped slot, while the mid segment realizes the overall movement of robot. In order to evaluate the design and implementation of the mobile robot platform, functional analysis is devoted to modules of robot. Especially for the requirements of walking stability on the V-shaped slot, creeping gait planning is analyzed to construct a multi-axis coordinating movement control scheme for creeping motion. Finally, by using the simulated EAST nuclear fusion vessel, the principle prototype is tested, and the preliminary evaluation of its functional index and related technical parameters is carried out. The experimental results show that the principle prototype of the robot can achieve stable walking on the V-shaped circular slot at the bottom of the nuclear fusion vessel, and it has a certain ability to carry equipments.

1. Introduction

The internal vessel of Experimental Advanced Superconducting Tokamak (EAST) is usually referred to as nuclear fusion vessel. The circular vessel of EAST is called D-shaped vessel with the vertical section like “D”. The first wall (PFCs) is the inner surface of the nuclear fusion vessel, with welded tiles made of stainless

* Corresponding author at: Institute of Intelligent Machines, Chinese Academy of Sciences, Hefei, Anhui 230031, China. Tel.: +86 551 65591337; fax: +86 551 65592420.
E-mail addresses: zhangqiang@iim.ac.cn (Q. Zhang), zfwang@ustc.edu.cn (Z. Wang).

http://dx.doi.org/10.1016/j.fusengdes.2017.03.054
0920-3796/

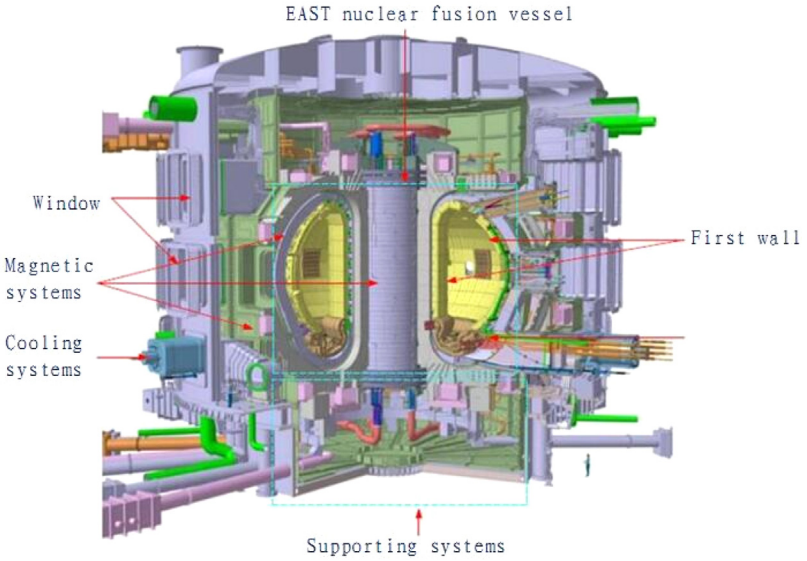

Fig. 1. Internal structure of ITER or EAST nuclear fusion vessel.

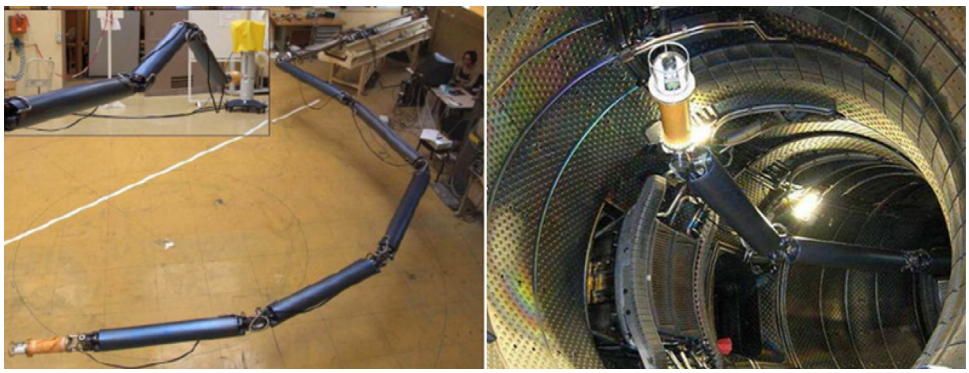

Fig. 2. Manipulator of Articulated Inspection Arm (AIA).

steel (ITER) or graphite (EAST), which can provide security for the safe operation of the nuclear fusion devices, as shown in Fig. 1. In daily operation, parts of the tiles of the first wall could be damaged by impact of high energy particles to affect the safety of the nuclear fusion. Therefore, regular maintenance of the first wall becomes an urgent demand of the normal experiment. Owing to the extreme physical environment of strong radiation, high temperature, intense magnetic field and high vacuum, it's required to carry out maintenance in the interval period of the nuclear fusion, in which there is still residual neutron radiation, so that the maintainers should not directly enter the vessel to operate the relevant parts. Therefore, it is necessary to replace the human by robots which can enter the vessel to fulfill the detection and maintenance tasks of the first wall by means of the remote control method [1–3].

The abroad existing research results for the detection and maintenance work in the nuclear fusion vessel reflects in the manipulator robots [4,5]. The CEA-LIST in France had successfully developed the Articulated Inspection Arm (AIA) in 2002. As shown in Fig. 2, it is modularly designed of 5 joints, with a vertical and a horizontal rotational DOF of each joint. The horizontal rotational motion is driven by a motor installed in the module, while the vertical rotational motion is driven by a motor installed in the parallelogram linkage. Motions are transmitted by wire ropes from the output axis of motors to the wheels of rotational joints, to drive the relative rotational motion between modules. The robot can closely observe the first wall of the vacuum vessel during the interval period of the physical experiment, and can monitor in real time the working conditions of Tokamak vacuum vessel during the operation period. However, its driving force devices are integrated inside the joints, which increase the arm weight, enlarge the burden of the robot arm and limit the total length and the work space for detection. Furthermore, the inherent structure of the manipulator robot determines that it has only limited detection function, but not maintenance operation. The OC Robotics in Britain had been researching a snake-like robot (shown in Fig. 3) since 2001. The snake-like robot is controlled by wire ropes getting through a group of active joints with perfect flexibility. The robot can bend as required and reach the point where other robots are unable to reach. The end of the robot can be installed with cameras, lamps, cutting equipments and so on, which is applied to do security checking, cleaning and maintenance in the nuclear radiation area. All of the driving force and transmission devices are located at the base end of the robot, and the base is installed on a heavy industrial manipulator. However, on the other hand, this structural scheme requires high capability, which could disturb the positioning accuracy and repositioning accuracy of the robot and cause the accumulative error to be larger. It is also not good for the integration and optimization of the control system. On the other hand, limited by the radial size and joint strength, the end of the robot is not suitable to carry heavy tools, which limits its application range.

The articulated dual manipulator robot platform studied by the JET team in Britain is a kind of remote system in vessel [6–9]. As

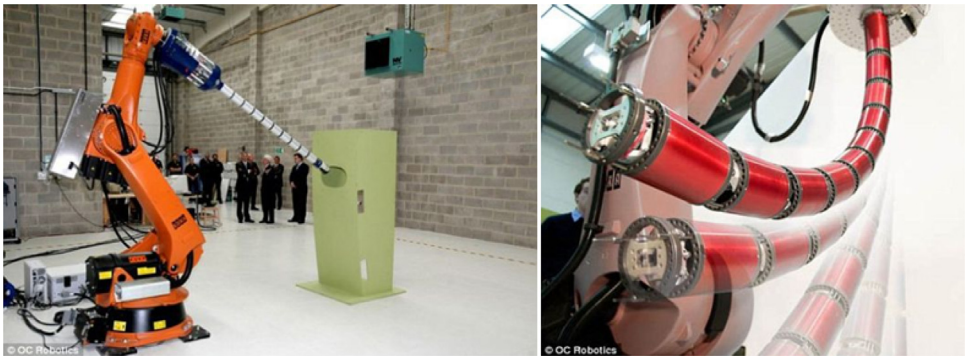

Fig. 3. Snake-like robot of OC Robotics.

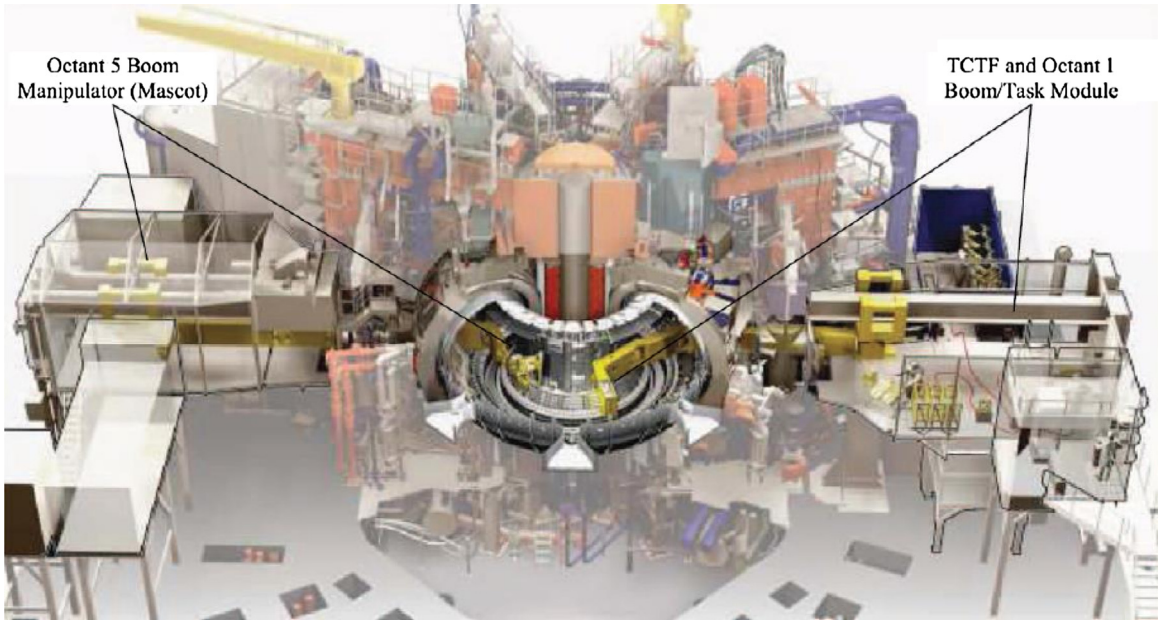

Fig. 4. JET vessel maintenance manipulator platform.

shown in Fig. 4, this system is constituted by a pair of linkage jointed manipulators. While the system is entering the circular vessel from the opposite sides in 180°, one arm delivers the tools and another operates to work in coordination. Due to the introduction of the tool system, the JET remote system can fulfill complicated tasks such as state detection, structure maintenance, and replacement of components, in order to solve the working problems in compact environments. However, the multifunction system leads to various problems such as huge physique, numerous parts, complicated structure and the resulting complex control system and high error rate. Based on JET, in view of the ITER, the Oxford group in Britain brings the concept of MPD, in order to achieve the broader remote performance capacity. It can accomplish sorts of operations except that of the package layer and major components of the partial filter in Tokamak, as shown in Fig. 5. In the design process of MPD, the kinematics of the manipulator, the reachable space, the storage and deployment of the vehicle, the failure recovery and various technical risks are comprehensively considered, thus to confirm the solution with the flexible manipulator appended to the major cart, the end operator, the remote operating tools, the tool conveying system, the control system and the remote viewing and illumination. Although the system has excellent operating performance, it still has a lot of shortcomings such as huge system, complicated structure, complex control flow and expensive manufacturing cost.

In the existing research results, a part of manipulator robots are limited by their inherent supporting strength, load weight and size space to do the jobs [10,11]. Robotic arm systems for remote operation such as JET and MPD can carry certain tools to complete a variety of operating tasks, but it is difficult to achieve the system which is very complex. Therefore, it is necessary to develop a mobile robot which has a certain ability to carry equipments or assist manipulator robots to complete the detection and maintenance tasks of the first wall in the EAST fusion vessel. The structure of the mobile robot should be relatively simple and easy to control in order to better serve the operating system of the nuclear fusion reactor [12].

In view of the insufficiency of existing research results, combining with the above actual demand, this paper presents a wormlike creeping mobile robot working inside the nuclear fusion vessel. This robot can move along the V-shaped circular slot inside the EAST nuclear fusion vessel. Based on the structure design and function analysis of modules, a principle prototype of wormlike creeping mobile robot is constructed, and basic movement properties and feasibility verification are completed. Furthermore, gait planning for wormlike creeping is researched to lay the theoretical foundation for the practical application of the robot.

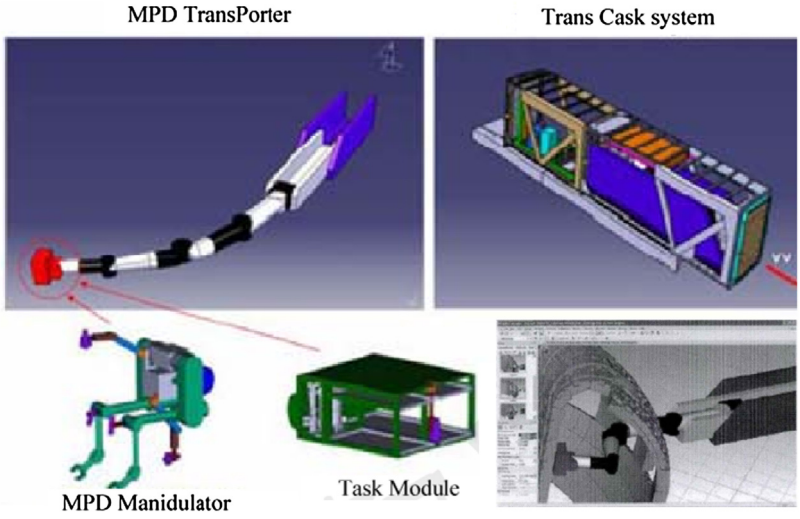

Fig. 5. MPD remote manipulator system.

2. Functional requirements and design points of the robot system

Scientific analysis of the working environment and design requirement can provide theoretical reference and guidance to the design of principle prototype. The functional requirements and design points are concluded as below:

(1) Operation conditions: It's during the interval period of nuclear fusion experiment, with no extreme condition of high temperature, high vacuum and intense magnetic field, but still with residue of neutron radiation.
(2) Geometric constraints and deployment: The geometric parameters and size of the vessel are large, e.g. in the EAST vessel, outer ring radius "R" is 1.94 m, and inner ring radius "r" is 0.45 m. Driven device is required to guide the robot get through the window of vessel and reach the bottom.
(3) Service object: The robot platform is to carry equipments or assist manipulator robots to complete the detection and maintenance tasks of the first wall, so the loading capability of manipulators is needed.
(4) Load: Since the weight of the normal operation tools is generally not more than 100 kg, the design standard of load is set to be 100 kg in this paper.
(5) Motion range: The manipulator is required to work in the whole vessel, with the motion range of robot platform covering the entire bottom of the vessel.
(6) Security: The robot should be able to operate safely and move steadily, not polluting or destructing the environment of the vessel.
(7) Structure characteristics: The robot is required to have simple structure and low manufacturing cost, which is easy to implement.
(8) Remote control performance: The robot should be remotely manipulated by a simple and convenient control method.

3. System design of the robot platform

3.1. Geometric constraints and deployment design

According to the functional requirements and design points of the robot platform, it is necessary to analyze the geometric constraint conditions of the motion of the robot in the vessel, and then to establish the supporting and bearing parts of the robot platform. It's a structured circular vessel with D-shaped section in the EAST fusion vessel, as shown in Fig. 6. The circular working space is horizontally symmetrical in the vessel, half bottom covered with graphite or stainless steel tiles in difference shapes such as L, V and W shaped section [3,13]. The L-shaped deck, the V-shaped deck and the W-shaped deck constitute the first wall. The L-shaped deck consists of vertical deck and horizontal deck. The vertical deck is as not suitable to support the weight of the robot as the horizontal deck scattered with obstacles. The W-shaped deck is too narrow at the deep end of the half bottom, with tiles easily damaged by external forces, which is also not suitable. The V-shaped deck is located at the middle of the half bottom, consisting of gentle slope decks between the wide gap on both sides, which is suitable to be the supporting base of the robot. In conclusion, the V-shaped deck is selected to be the supporting and bearing parts of the mobile robot platform. The working space between inside and outside of the V-shaped deck forms a V-shaped slot.

After establishing the supporting and bearing parts of the robot platform, it is necessary to deploy a reasonable path to ensure that the robot can enter the vessel from the outside during the interval period of the nuclear fusion experiment. As shown in Fig. 7, the deployment system consists of a pulling cart, a wire rope connection, a supporting track, a guiding device and a storage cabin. While the robot is up to enter the vessel, it is driven by the pulling cart through the wire rope connection to move along the supporting track, then the robot can go into the guiding device at the window and go onto the V-shaped slot of the vessel by the guiding device. Conversely, while the robot finishes the work to exit the vessel, it is driven by the pulling cart through the wire rope connection to move reversely along the V-shaped slot, then the robot can go onto the supporting track at the window, and go into the storage cabin along the supporting track. Horizontal rotation joints and vertical rotation joints are designed between the wire rope connection and the pulling cart, thus to control the moving direction of the robot while getting through the guiding device. The power supply, the cable winding engine and the motion control system are integrated on the pulling cart to ensure the remote control work. The entire path deployment task is performed in the storage cabin.

3.2. Selection of the motion form and establishment of the structure scheme

General mobile robots according to the different walking style can be divided into legging, jumping, creeping, wheeled and tracked

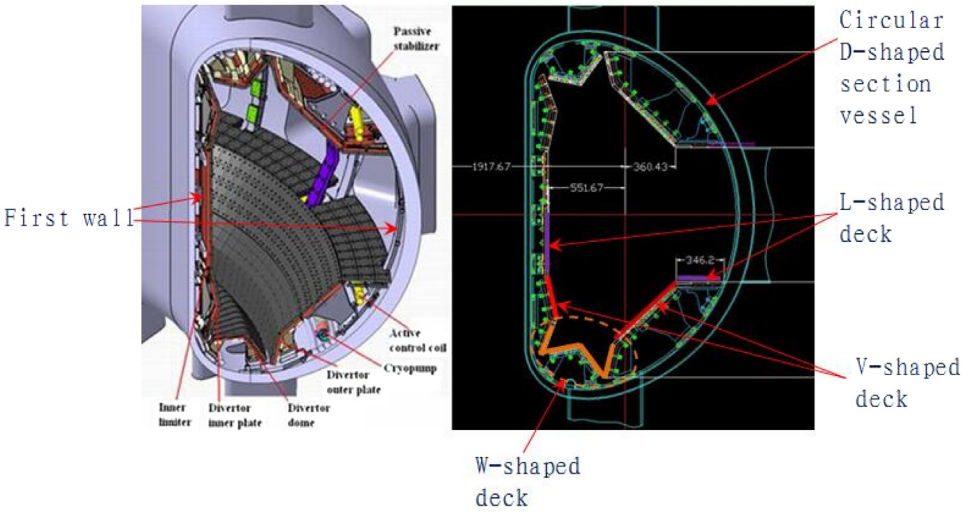

Fig. 6. Inner structure inside the EAST nuclear fusion vessel.

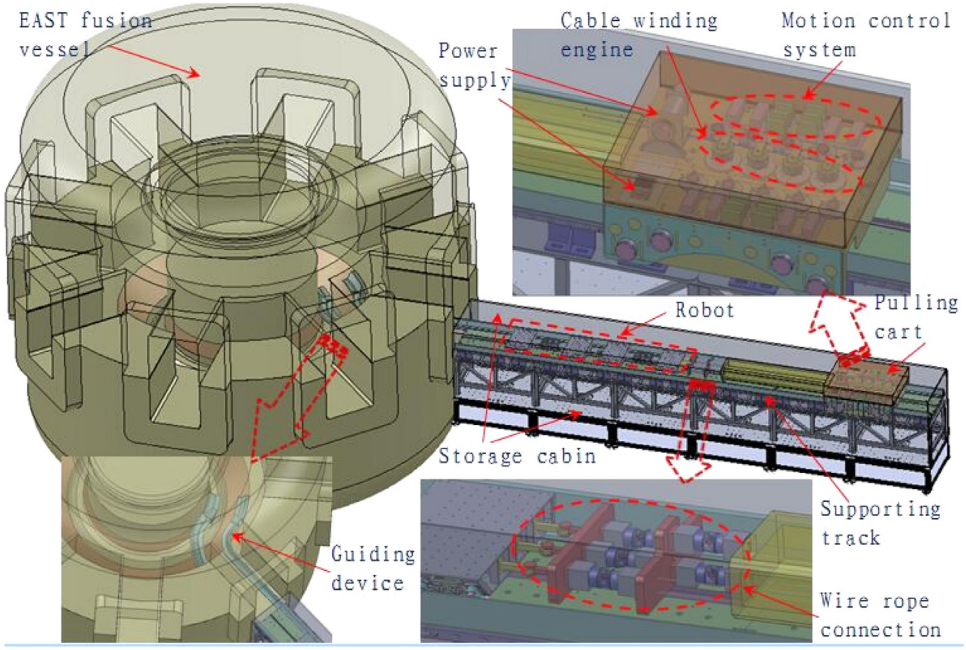

Fig. 7. Deployment system of the robot.

types. Facing the irregular structured operation environment of the EAST nuclear fusion vessel, the creeping scheme is one of the most stable and adaptable gaits in many types of motion mechanisms [14]. Meanwhile, as a base platform for carrying operation tools with a certain weight, the robot platform should be better to carry equipments or assist manipulator robots to complete the detection and maintenance tasks in the vessel, with good reconfigurability and versatility. Thus, multi-section structure is adopted on the robot, as shown in Fig. 8.

The mobile robot adopts chain structure, which is in series of n ($n \geq 2$) creeping units connected by telescopic elastic linkages. Each creeping unit is of three-part structure, which consists of a fore segment, a mid segment and a back segment connected by bidirectional universal joints. The fore and back segments have the same structure, symmetric at the two sides of the mid segment, stretching the paws to contact the V-shaped deck to control the lock/unlock state from the V-shaped deck. The mid segment is connected with the fore segment and the mid segment by the bidirectional universal joint to control feed expansion periodically. The coordinated motion between the fore, the mid, and the back seg-

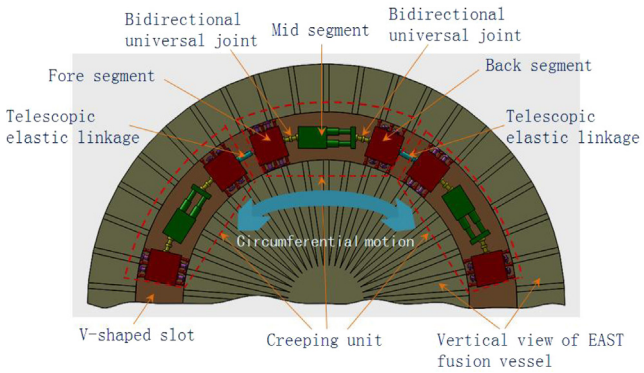

Fig. 8. Total structure of the mobile robot.

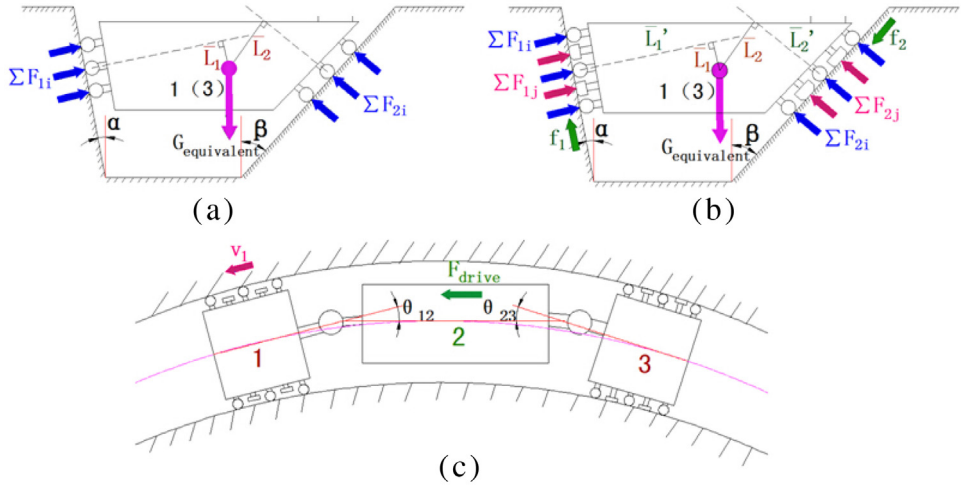

Fig. 9. Mechanical performance analysis of the robot.

ment can drive the single creeping unit move along the V-shaped slot in a wormlike style. Then the coordinated units constitute the wormlike creeping mobile robot [15].

3.3. Mechanical performance analysis of the robot

Mechanical performance analysis of the robot is necessary to be built as the important theory basis of engineering prototype, including the mechanical equilibrium conditions derivation of the fore/back segment in the lock/unlock state, and the dynamic performance analysis of the mid segment [16]. The fore, mid, back segment are marked with 1,2,3 respectively.

As shown in Fig. 9(a), while the paws on both sides keep retracting, the mechanical balance of segment 1 or 3 should meet the following conditions:

Force balance conditions: $\sum F_{1i}\sin\alpha + \sum F_{2i}\sin\beta = G_{equivalent}$, $\sum F_{1i}\cos\alpha = \sum F_{2i}\cos\beta$.

Moment balance conditions: $\Sigma F_{1i}\bar{L_1} = \Sigma F_{2i}\bar{L_2}$. Thereinto, $\sum_{1i} F_{1i} = \sum k_1\ \triangle x_{1i}$, $\sum F_{2i} = \sum k_2\ \triangle x_{2i}$.

As shown in Fig. 9(b), while the paws on both sides keep stretching and contacting the V-shaped deck, the mechanical balance of segment 1 or 3 should meet the following conditions:

Force balance conditions: $(\sum F_{1i} + \sum F_{1j})\sin\alpha + (\sum F_{2i} + \sum F_{2j})\sin\beta + f_1\cos\alpha = G_{equivalent} + f_2\cos\beta$, $(\sum F_{1i} + \sum F_{1j})\cos\alpha = (\sum F_{2i} + \sum F_{2j})\cos\beta + f_1\sin\alpha + f_2\sin\beta$.

Moment balance conditions: $(\Sigma F_{1i} + \Sigma F_{1j})\bar{L_1} + f_1\bar{L_1'} + f_2\bar{L_2'} = (\Sigma F_{2i} + \Sigma F_{2j})\bar{L_2}$. Thereinto, $\sum F_{1i} = \sum k_1\ \triangle x_{1i}$, $\sum F_{2i} = \sum k_2\ \triangle x_{2i}$, $f_1 = \mu_0' \sum F_{1j}$, $f_2 = \mu_0' \sum F_{2j}$.

As shown in Fig. 9(c), in order to ensure segment 2 creep steadily on the V-shaped slot in the coordination of segment 1 and 3, the mechanical balance should meet the following conditions:

$F_{drive}\cos\theta_{12} > \mu_{10}\ (\sum F_{1i} + \sum F_{2i})$, $F_{drive}\cos\theta_{23} < \mu'_{30}\ (\sum F_{1j} + \sum F_{2j})$. Thereinto, $\sum F_{1i} = \sum k_1\ \triangle x_{1i}$, $\sum F_{2i} = \sum k_2\ \triangle x_{2i}$.

In the above formulas, the meaning of each mathematical symbol is shown in Table 1. Where $\triangle x_{1i}$, $\triangle x_{2i}$ could make small change following the adjustment of the orientation of segment 1 and 3, to keep the balance state of the system.

4. Structure design and function analysis of the composition modules of the robot

4.1. Design of the fore/back segment

The fore/back segment is the lateral positioning module of the robot, constituted with the supporting submodule, the driving submodule, the inward stretching submodule, the outward stretching submodule and the loading platform. As shown in Fig. 10(a) and (b), the driving submodule is installed in the supporting submodule, the inward/outward stretching submodule is set symmetrically at both sides of the supporting submodule in the same structure, one end connected with the driving submodule, another end stretching over the supporting submodule, which constitute the shearing extension mechanism. The driving submodule consists of a ball screw mechanism driven by a vacuum servo motor, driving the inward/outward stretching submodule on both sides stretching out and back synchronously to control the lock/unlock state from the V-shaped slot, as shown in Fig. 11. The supporting submodule is for the whole segment supporting, with inverted wedge-shaped section. The normal direction of the inward and outward end face, on which installed n ($n \geq 2$) sets of linear uniformed rollers as the supporting end of fore/back segment, is paralleled with the normal direction of the V-shaped deck. On the one hand, it is beneficial to increase the contact area and ensure uniform stress. On the other hand, it can improve the bearing performance of the fore/back segment. Each roller keeps the same direction with the tangential direction of the circular vessel, and the roller is constraint to roll at the radial direction in order to prevent skidding and to ensure the accuracy of motion position. Each roller has a spherical hinge and a sliding fit driven by a spring, which improves its self-adaptive ability while moving across the damaged deck. Furthermore, the rollers can minimize the friction resistance between the robot and the deck, optimize the system driving performance, and achieve the goal of saving energy consumption. However, note that since the fore/back segment is always in contact with the surface of the V-shaped circular slot, under the condition of heavy load, the paws and rollers may cause slight damage to the surface of the graphite or the stainless steel tile on the surface of the V groove during the process of movement, which needs to be further explored in the future optimization design.

As shown in Fig. 10(a), there is a loading platform installed on the upper plane of the supporting submodule. The loading platform has a dual role to install equipments or manipulator robots with a certain weight upon the upper surface and seal the electronic hardware of the control system inside, as shown in Fig. 9.

4.2. Design of the mid segment

The mid segment is the circumferential motion module of the robot, constituted with the supporting submodule, the fore submodule and the back submodule, as shown in Fig. 12. The fore

Table 1
Specific meanings of the mathematical symbols in the mechanical balance formulas.

Mathematical symbol	Specific meaning
F_{drive}	the feed force that drive the telescopic motion between the segment 1 and 3
$\sum F_{1i}$	the counter force of V-shaped deck to the rollers of segment 1
$\sum F_{2i}$	the counter force of V-shaped deck to the rollers of segment 3
$\sum F_{1j}$	the counter force of the V-shaped deck to the paws of segment 1
$\sum F_{2j}$	the counter force of the V-shaped deck to the paws of segment 3
f_1	the static friction between the V-shaped deck and the paws of segment 1
f_2	the static friction between the V-shaped deck and the paws of segment 3
k_1	the elastic coefficient of springs in inward rollers
k_2	the elastic coefficient of springs in outward rollers
$\triangle x_{1i}$	the compression deformation of springs in inward rollers
$\triangle x_{2i}$	the compression deformation of springs in outward rollers
μ_0'	the static friction coefficient between the V-shaped deck and the paws
μ_{10}	the rolling friction coefficient between the V-shaped deck and the rollers of segment 1
$\mu_{'30}$	the static friction coefficient between the V-shaped deck and the paws of segment 3
$G_{equivalent}$	the equivalent gravity of segment 1 or 3 when carrying a certain operating device
$L_{\overline{1}}$	the equivalent arm of the force of $(\sum F_{1i} + \sum F_{1j})$ to the center of the gravity of segment 1 or 3
$L_{\overline{2}}$	the equivalent arm of the force of $(\sum F_{2i} + \sum F_{2j})$ to the center of the gravity of segment 1 or 3
$L_{\overline{1}}'$	the equivalent arm of the force of f1 to the center of the gravity of segment 1 or 3
$L_{\overline{2}}'$	the equivalent arm of the force of f2 to the center of the gravity of segment 1 or 3
α	the angle between the vertical plane and the tangent plane of inward deck
β	the angle between the vertical plane and the tangent plane of outward deck
θ_{12}	the angle between the vertical middle section of segment 2 and the vertical middle section of segment 1
θ_{23}	the angle between the vertical middle section of segment 2 and the vertical middle section of segment 3

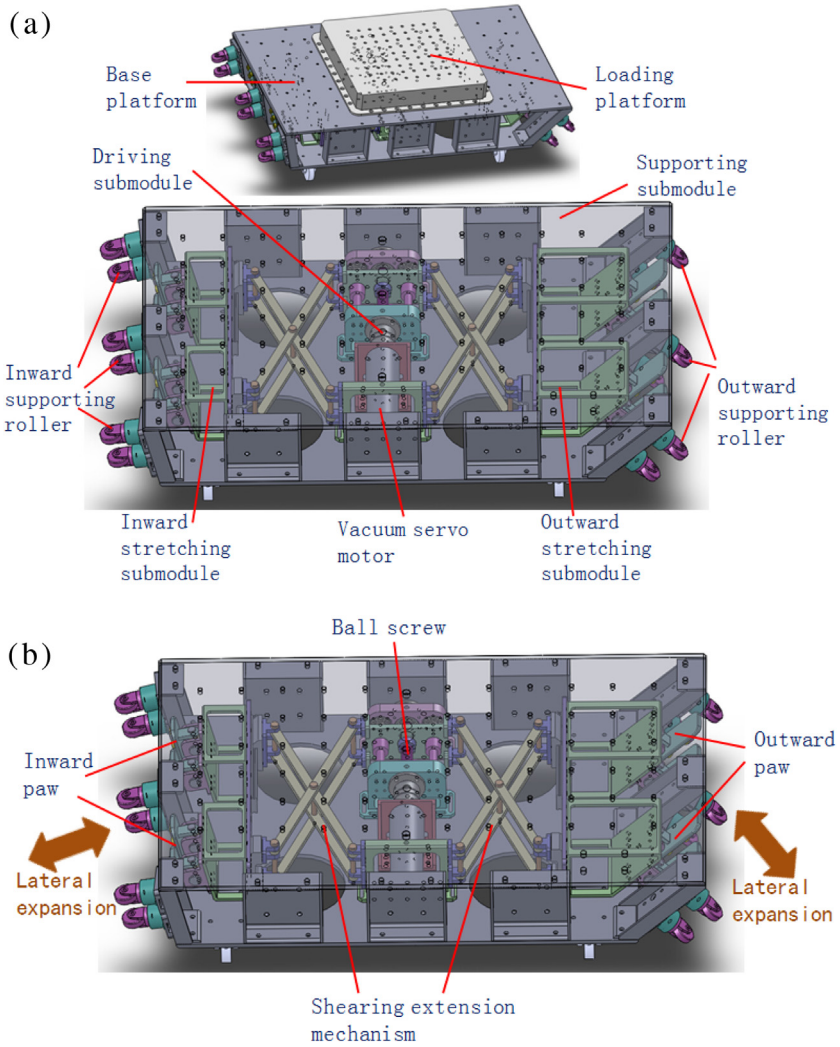

Fig. 10. (a) Structure of the fore/back segment. (b) Structure of the fore/back segment.

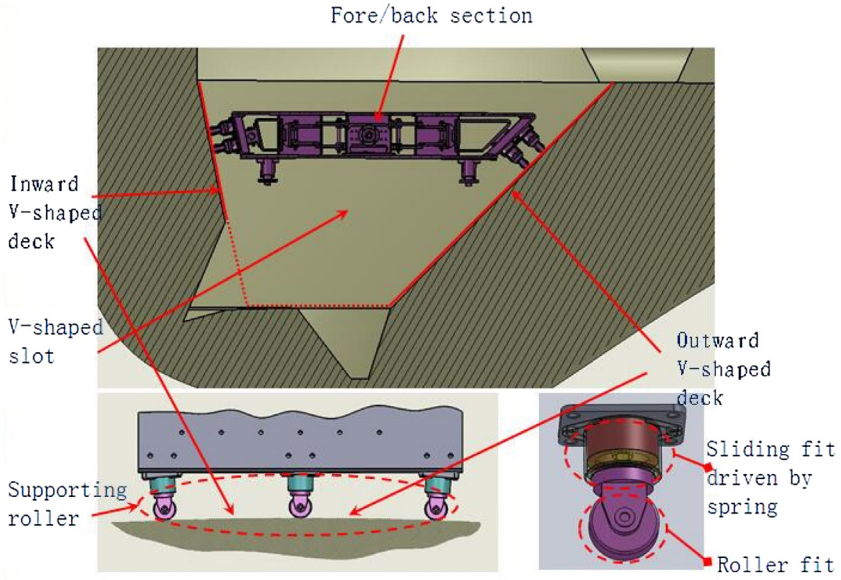

Fig. 11. Fore/back segment located on the V-shaped slot.

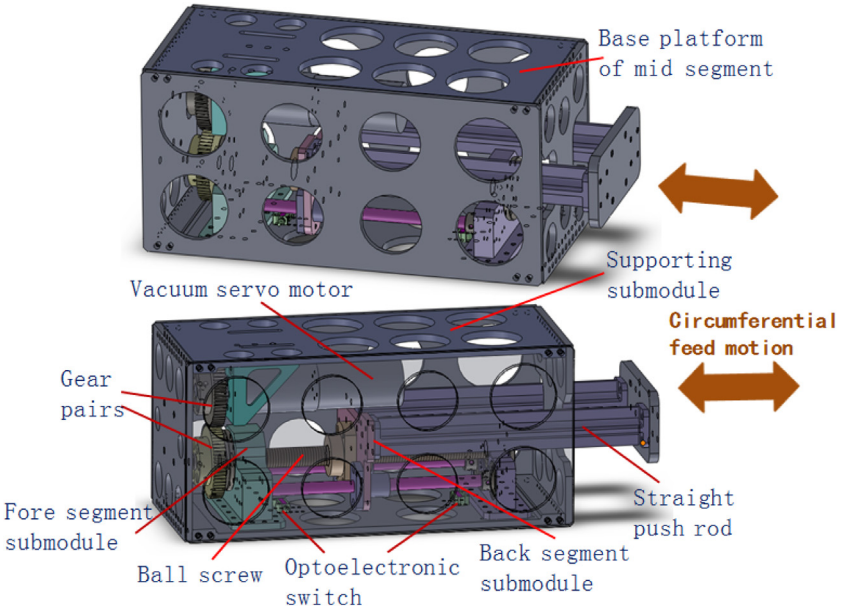

Fig. 12. Structure of the mid segment.

submodule is installed inside the supporting submodule. The fore submodule and the back submodule move relatively along the axis direction as an elastic whole. The supporting submodule is the supporting frame assembled of rectangular plates. A vacuum servo motor installed in the supporting submodule drives the gear pairs transmitting to a ball screw, and then transmitting to a straight push rod, realizing the relative feed motion between the fore submodule and the back submodule. Inside the supporting submodule, two optoelectronic switches are installed to sense the position variation of the straight push rod, and they respectively give the position signal of two extreme positions to the robot control system in order to precisely control the periodic feeding distance of the mid segment. The gear pairs are designed for power transmission and for shortening the length of the mid segment in order to increase the through capacity of the robot on the circular V-shaped slot.

4.3. Design of the bidirectional universal joint and the telescopic elastic linkage

The bidirectional universal joint and the telescopic elastic linkage are the connecting modules of the robot. As shown in Fig. 13, the bidirectional universal joint is for connection between the fore/back and the mid segment within each creeping unit. Jointed cross joints consist the bidirectional universal joint, with two dimension rotations. Comparing with the single universal joint, the bidirectional universal joint cannot only efficiently adapt the variation of the supporting force and the gravity center but also dynamically adjust the relative position between the mid segment and the fore/back segment. . Installing sorts of operation tools, the robot has a certain practicability to carry equipments or assist manipulator robots to complete the detection and maintenance tasks inside the vessel. The running condition of the robot on the V-

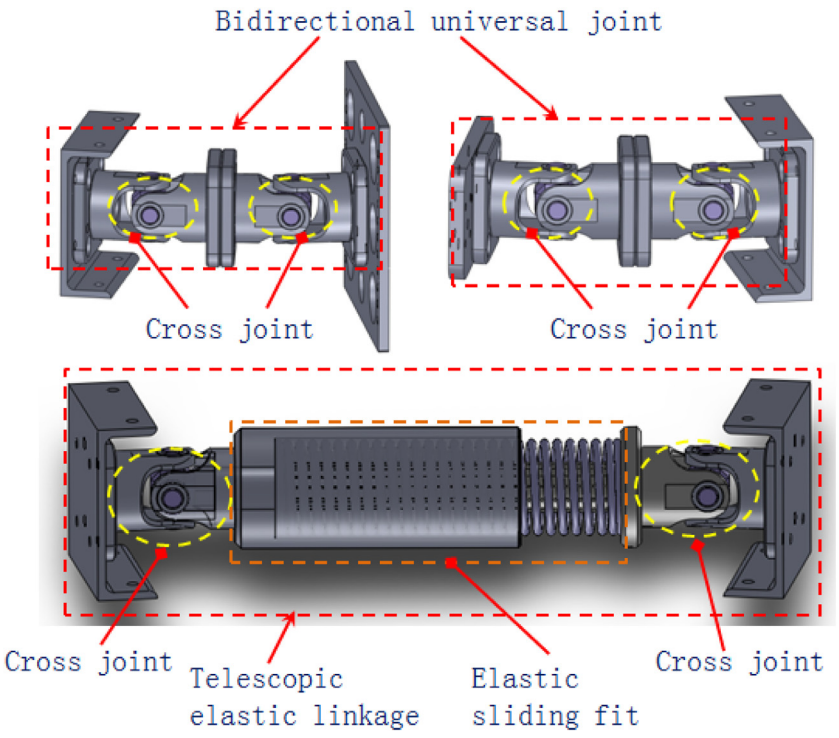

Fig. 13. Structure of the connecting module.

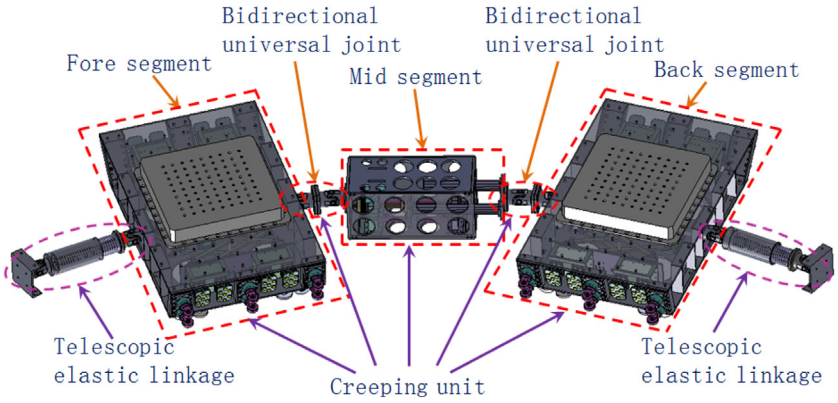

Fig. 14. Structure design of the wormlike creeping mobile robot.

shaped slot inside the EAST nuclear fusion vessel is shown in Fig. 15. Fig. 16

The telescopic elastic linkage is for the connection between neighboring creeping units, with three sections connected with cross joints. The mid section is an elastic sliding fit with spline and spring, while connecting creeping units to be the unified whole and coordinating the gait of creeping units with the elastic motion. The maximum telescopic distance is no less than the maximum feed moving distance of the mid segment in order to prevent mechanical interference. While creeping on the V-shaped slot, the fore/back segment of each creeping unit does the lock/unlock motion, and the mid segment does the telescopic motion, and the telescopic elastic linkage between units does the corresponding telescopic motion.

4.4. Composite design of the modules

The mid segment and the fore/back segment connected with the bidirectional universal joints mentioned above form a creeping unit. At least two creeping units connected with telescopic elastic linkages form a chained wormlike creeping mobile robot, as shown in Fig. 14 shows two typical applications of the robot platform. Fig. 16(a) shows the robot platform carrying a parallel visual detection device, while Fig. 16(b) shows the robot platform carrying a kind of two-dimensional mobile device assisting the manipulator robot to carry out maintenance operation.

Here it is worth noting that, in the above structure design of each functional module, the operating conditions of the robot are based on the intermittent period of the nuclear fusion experiment, which only take into account the geometric constraint and residual nuclear radiation, ignoring the working temperature and the vacuum degree limit. However, there is still a certain degree of high temperature and vacuum environment in the vessel, so the structure design of the robot needs to be supplemented and optimized. For example, it is necessary to consider the thermal control system design of the electromechanical devices of the robot in the next step. The main body of the robot is made of aluminum alloy(6061-T6), which needs to be replaced by a high temperature resistant

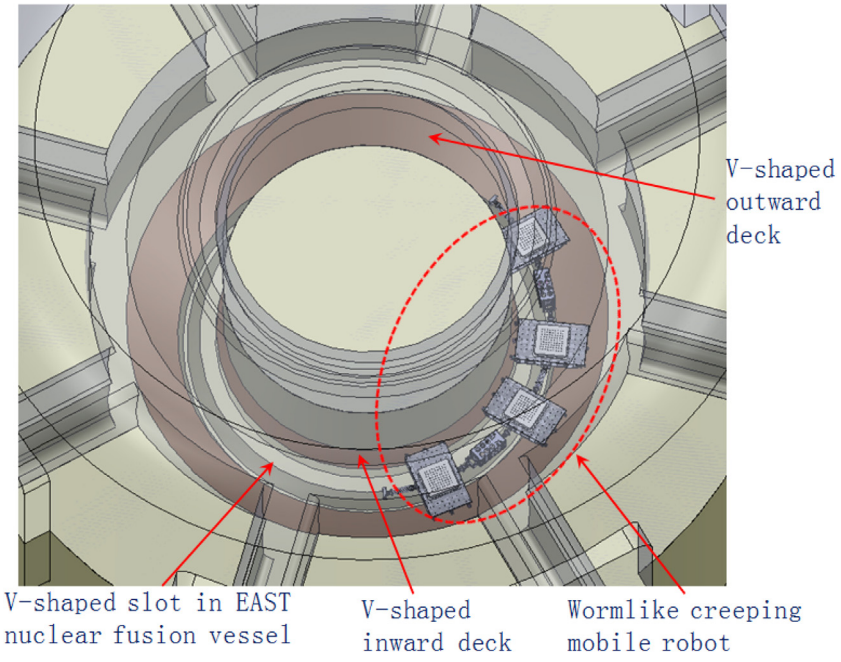

Fig. 15. Running condition of the robot on the V-shaped slot.

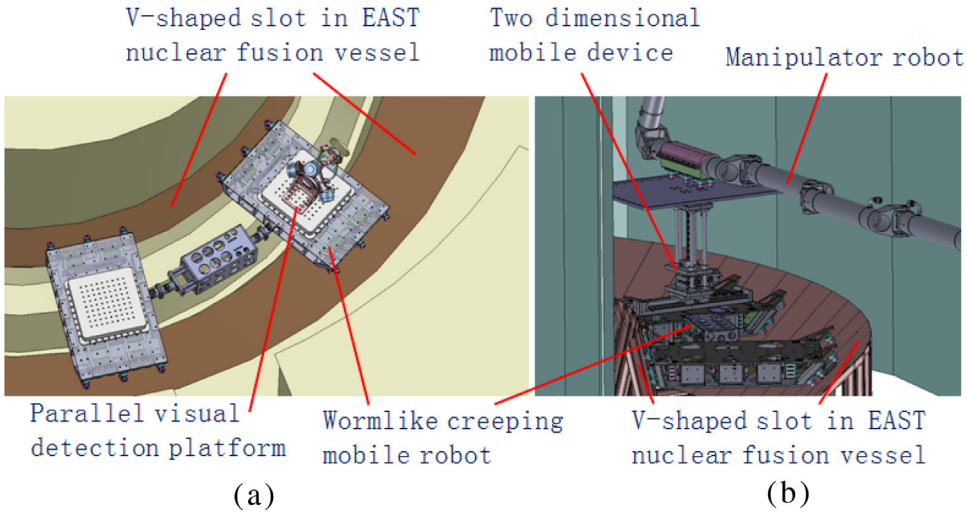

Fig. 16. Two typical applications of the robot platform.

titanium alloy. The problems of sealing and vacuum lubrication of the robot body parts are still to be solved.

5. Analysis of the motion gait planning and construction of the control scheme

To ensure the robot could move steadily on the V-shaped slot, a reasonable analysis of motion gait planning and time series is required. Based on this, a suitable motion control scheme is constructed [15,17]. The wormlike creeping mobile mechanism is based on the mutual coordination between the fore/back and the mid segment, belonging to a periodical gait. In order to illustrate easily, the fore segment, the mid segment and the back segment are marked in number 1, 2 and 3 respectively, the telescopic elastic linkage is marked in number 4.

In the segment 1 and 3, the vacuum servo motor drives each ball screw transmission to do a reciprocating motion, setting the revolution of the motor output shaft corresponding to one stroke as n_1. In the segment 2, the vacuum servo motor drives the ball screw transmission to do a reciprocating motion, setting the revolution of the motor output shaft corresponding to one stroke as n_2. According to the different motion state of the segment 1, 2 and 3, the time cost of one creeping step, which is clockwise in overhead view, is set as one period $T(0 < t_1 < t_2 < t_3 < t_4 < t_5 < T)$. In each period of time within one period T, the steps are controlled in Table 2. The state of each typical time point is shown in Table 3.

Thus, the robot completes an entire period of one clockwise step on the V-shaped slot, as shown in Fig. 17. The anticlockwise step is similar to the clockwise step, merely the rotation direction of the motor and the control sequence are different.

Figs. 18 and 19 show the motor control state of the creeping period and the corresponding stretching state of the modules, corresponding to the gait pattern in Fig. 17. The horizontal axis denotes the time phase in period 0∼T, the vertical axis in Fig. 18 denotes the motor control state of the segment 1, 2 and 3, and the vertical axis in Fig. 19 denotes the stretching state of the segment 1, 2,3

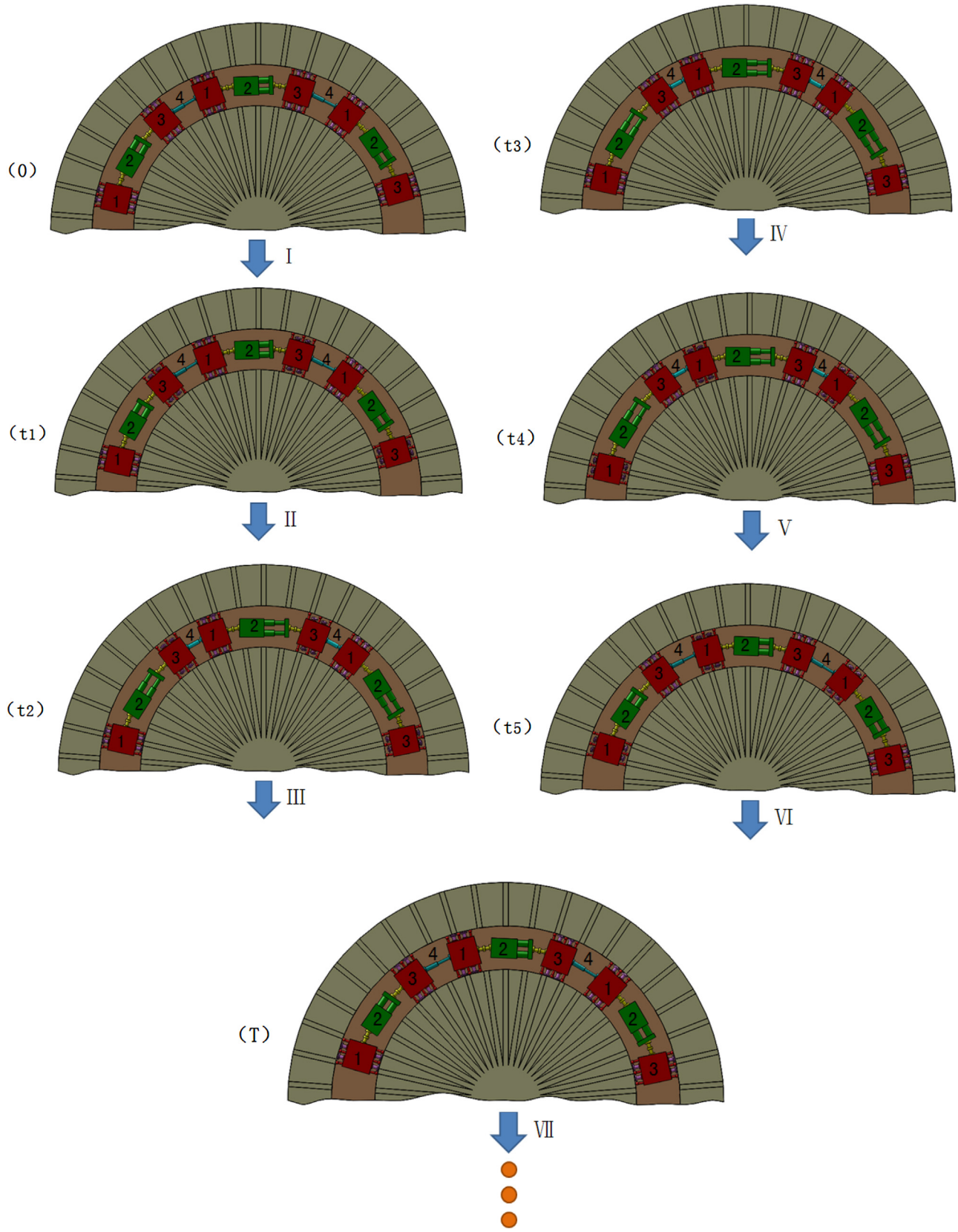

Fig. 17. Gait planning and analysis of the wormlike creeping movement on the V-shaped slot.

and telescopic elastic linkage 4. "$+R\frac{n_1}{2}$", "S", and "$-R\frac{n_1}{2}$" in Fig. 18 respectively denote that the motors in segment 1 and 3 rotate forward $n_1/2$, stop, and rotate backward $n_1/2$; "$+R\frac{n_2}{2}$", "S"', "$-R\frac{n_2}{2}$" in Fig. 18 respectively denote that the motor in segment 2 rotates forward $n_2/2$, stops, and rotates backward $n_2/2$. In Fig. 19, for the fore/back segment, "+","−" respectively denote the maximum and minimum stretching state of the paws. For the mid segment, "+", "−" respectively denote the maximum and minimum stretching

Table 2
Action changes of each segment of the robot in each period of time within one period T.

Movement change	Fore segment 1		Mid segment 2		Back segment 3		Telescopic elastic linkage 4
Time scale	Motor	Paws	Motor	Submodles	Motor	Paws	
$0–t_1$	stop	stretch longest	stop	keep relative rest	rotates forward $n_1/2$	retracting back	keeps maximum extended
$t_1–t_2$	stop	stretch longest	rotates forward $n_2/2$	back submodule moving one step towards the right	stop	retract shortest	shortens until the minimum
$t_2–t_3$	stop	stretch longest	stop	keep relative rest	rotates backward $n_1/2$	Stretching out	keeps minimum shortened
$t_3–t_4$	rotates forward $n_1/2$	retracting back	stop	keep relative rest	stop	stretch longest	keeps minimum shortened
$t_4–t_5$	stop	retract shortest	rotates backward $n_2/2$	fore submodule moving one step towards the right	stop	stretch longest	extends until the maximum
$t_5–T$	rotates backward $n_1/2$	Stretching out	stop	keep relative rest	stop	stretch longest	keeps maximum extended

Table 3
State of each segment of the robot at each typical time point within one period T.

State	Fore segment 1	Mid segment 2	Back segment 3	Telescopic elastic linkage 4
Time point				
0	locked	minimum shortened	locked	maximum extended
t_1	locked	minimum shortened	unlocked	maximum extended
t_2	locked	maximum extended	unlocked	minimum shortened
t_3	locked	maximum extended	locked	minimum shortened
t_4	unlocked	maximum extended	locked	minimum shortened
t_5	unlocked	minimum shortened	locked	maximum extended
T	locked	minimum shortened	locked	maximum extended

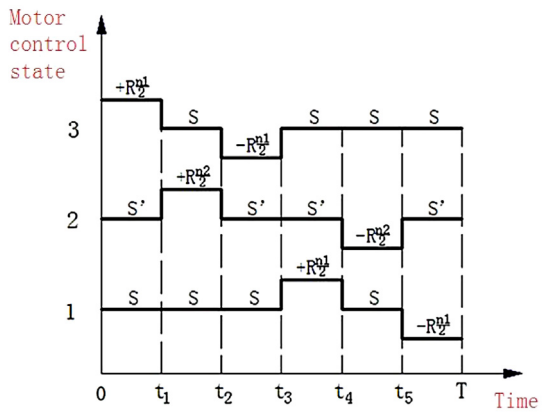

Fig. 18. Motor control state of the creeping period.

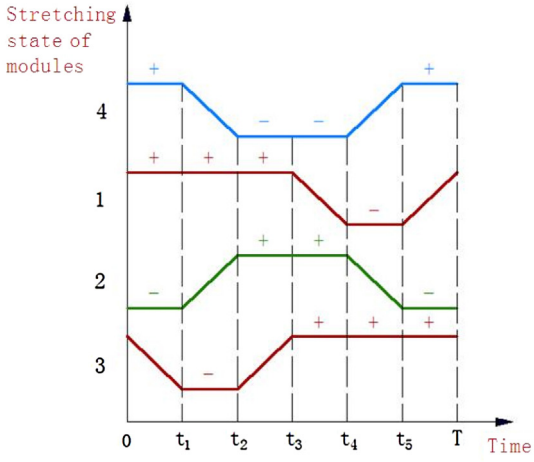

Fig. 19. Stretching state of the modules varying with time.

state of the submodules. For the telescopic elastic linkage, "+", "–" respectively denote the maximum and minimum stretching state of the linkage. The rising and falling slash denote the states between extreme states.

The motor control system chart is shown in Fig. 20. The motion gait of the creeping units is coordination controlled by the multi-axis controller, and the segments in each creeping unit are controlled by each motor driver. Power module is for power supply of the electromechanical module. The EtherCAT protocol is adopted to communicate between the multi-axis controller and the motor drivers.

6. Development of the principle prototype and test of the basic movement performance of the robot

6.1. Development of the principle prototype

Based on the system scheme design, the modular structure design, the function analysis and the motion gait planning, the mechanical and electrical components of the robot are manufactured and assembled. The principle prototype and the movement control hardware system are constructed. Meanwhile, a set of geometric devices, whose manufacturing material is tentatively designed as stainless steel with black paint on the surface, for simulating the environment of the V-shaped slot at the bottom of the EAST nuclear fusion vessel are built [3,18], as shown in Fig. 21.

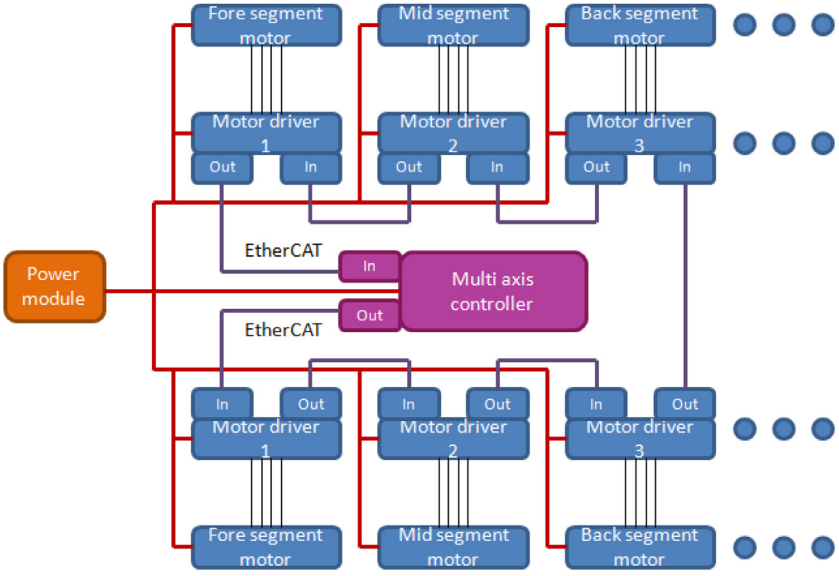

Fig. 20. Motor control system chart.

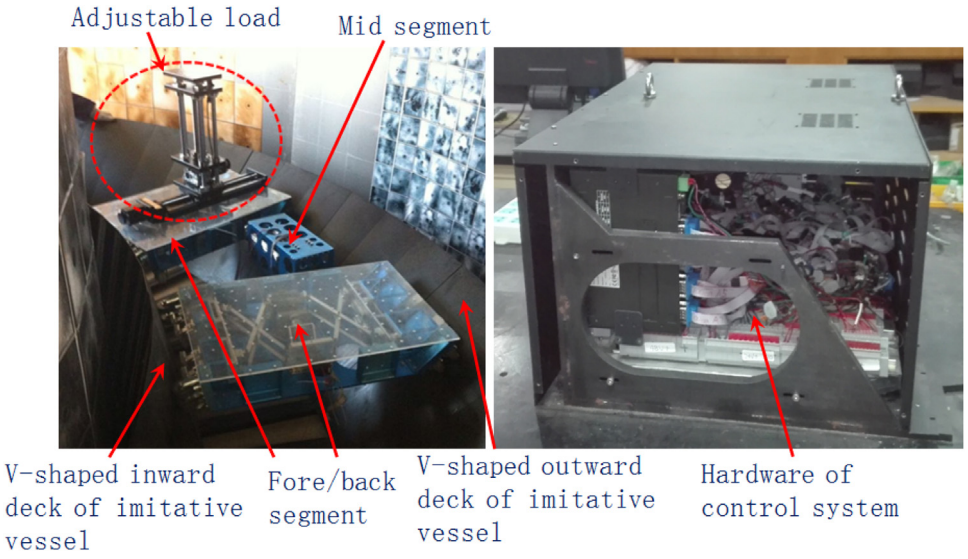

Fig. 21. Principle prototype of the robot.

The main technical indexes of the principle prototype are shown in Table 4. It needs to be explained that due to the limitation of the current research and development costs, the main technical indexes of the principle prototype are only for one creeping unit, and the development process of the prototype for multiple creeping units needs to be completed for the next step.

6.2. Basic movement performance test

As shown in Fig. 22, the principle prototype is set on the imitative V-shaped slot of the EAST nuclear fusion vessel in order to evaluate and verify the basic motion performance and mechanical properties of the wormlike creeping mobile robot [19]. The test experiment is carried out according to the following steps:

Firstly, measuring weights of 0 kg, 10 kg, 20 kg, 30 kg, 40 kg are respectively added at the middle position on the loading platform whose self-weight is 10 kg of the fore and back segment, to test the basic static load capacity of the robot, as shown in Fig. 22(a)and (b).

Secondly, measuring weights of 40 kg are respectively added at A/B/C/D/E five different positions with a radial uniform spacing of 100 mm on the loading platform whose self-weight is 10 kg of the fore and back segment, to test the offset static load capacity of robot, as shown in Fig. 22(c).

Thirdly, measuring weights of 40 kg are added at the middle position on the loading platform whose self-weight is 10 kg of the fore and back segment, and the corresponding motion control program is compiled at the same time,to test the basic motion performance and dynamic load capacity of the robot, as shown in Fig. 22(d).

As shown in Fig. 22(e),power-on test of each motor of the segment 1, 2,3 is carried on, timing for 3 min. In this process, the space coordinates of the marker point M located at the middle position on the mid segment are precisely tracked by a laser rangefinder, and the moving distance of the marker M in each stage of the periodic stretching motion is calculated. At the same time, the starting and ending time point of each periodic stretching action of each module are accurately recorded by a digital millisecond table with

Table 4
Main technical indexes of the principle prototype.

A creeping unit of the robot	Total weight	≤40 kg
	Dimensions (L × W × H)	1300 mm × 700 mm × 150 mm
	Mean creeping speed	≥0.5 m/min
	Rated load	100 kg
	Positional accuracy	≤2 mm
	Maximum relative error of one creeping period	≤0.5%
Fore/back segment (Lateral positioning module)	Main manufacturing material	aluminum alloy 6061-T6
	Weight	14 kg
	Dimensions (L × W × H)	400 mm × 700 mm × 90 mm
	Motor power	150 W (planetary reducer 75:1)
	Major parameters of the ball screw	diameter 14 mm, lead 2 mm
	The lateral stretching distance of the paws	100 mm
Mid segment (Circumferential motion module)	Main manufacturing material	aluminum alloy 6061-T6
	Weight	8.5 kg
	Dimensions (L × W × H)	300 mm × 150 mm × 150 mm
	Motor power	150 W (planetary reducer 75:1)
	Major parameters of the ball screw	diameter 16 mm,lead 32 mm
	Circumferential stretching distance	200 mm
Bidirectional universal joint (Connecting module)	Manufacturing material	stainless steel 304
	Weight	1.5 kg
	Rotation angle	horizontal deflecting ±45°, vertical pitching ±45°

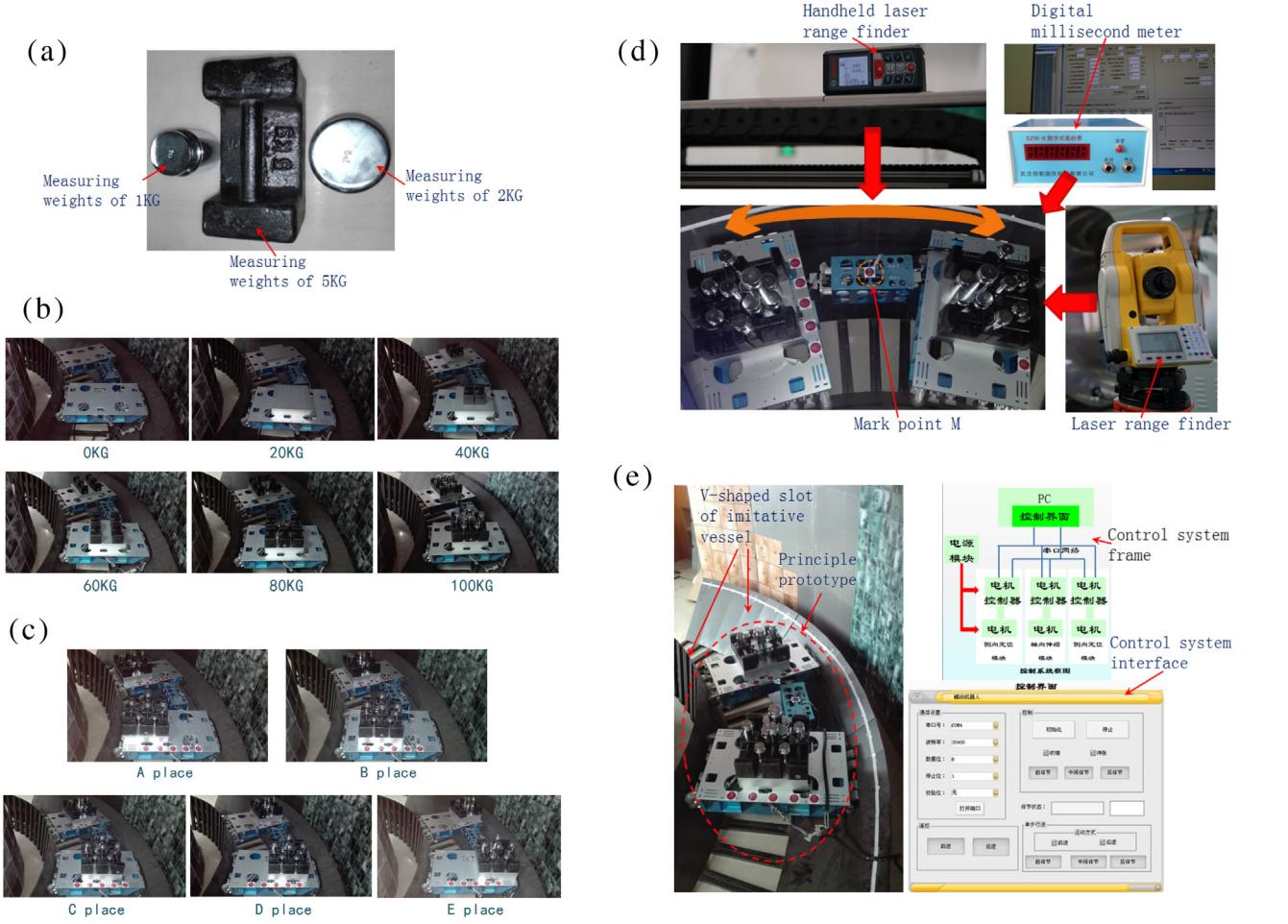

Fig. 22. (a) Combination of measuring weights of 1 kg, 2 kg and 5 kg. (b) Test of the basic static load capacity of the robot. (c) Test of the offset static load capacity of the robot. (d) Test of the basic motion performance and dynamic load capacity of the robot. (e) Basic movement performance experiment of the robot creeping on the imitative V-shaped slot.

the precision round up to 10 ms, and the expansion state charts of modules are drawn, as shown in Fig. 23. Then, the actual running cycle and the actual moving distance of the mark point M of each creeping step are calculated. By comparing the actual value with the theoretical value, we can calculate the maximum relative error of creeping period and the model positioning accuracy based on the mark point M, so as to verify the feasibility of the operation of the robot system.

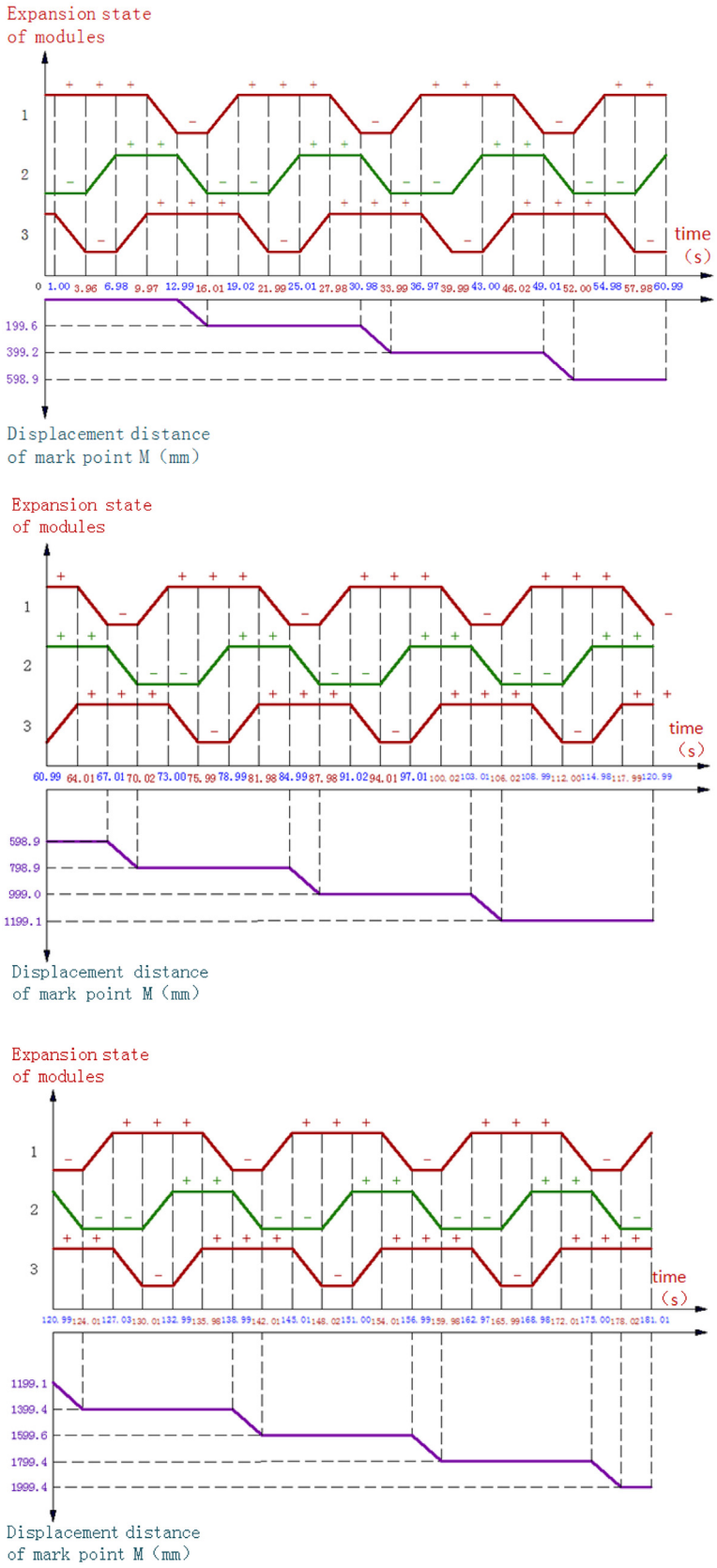

Fig. 23. Expansion state of modules and moving distance of the mark point M varying with time.

Table 5
Experimental results of the relative errors of creeping period.

Step order	Initial test time point (s)	End test time point (s)	Actual creeping period (s)	Theoretical creeping period (s)	Absolute error (s)	Relative error	Accumulative time error/Time control precision (s)
1	1.00	19.02	18.02	18	0.02	0.11%	0.01
2	19.02	36.97	17.95	18	−0.05	0.28%	
3	36.97	54.98	18.01	18	0.01	0.06%	
4	54.98	73.00	18.02	18	0.02	0.11%	
5	73.00	91.02	18.02	18	0.02	0.11%	
6	91.02	108.99	17.97	18	−0.03	0.17%	
7	108.99	127.03	18.04	18	0.04	0.22%	
8	127.03	145.01	17.98	18	−0.02	0.11%	
9	145.01	162.97	17.96	18	−0.04	0.22%	
10	162.97	181.01	18.04	18	0.04	0.22%	

Table 6
Experimental results of the model positioning accuracy based on the mark point M.

Step order	Accumulated moving distance of the mark point M (mm)	Actual moving distance of the mark point M (mm)	Theoretical moving distance of the mark point M (mm)	Absolute error (mm)	Accumulative error/Model positioning accuracy (mm)
1	199.6	199.6	200	−0.4	−0.6
2	399.2	199.6	200	−0.4	
3	598.9	199.7	200	−0.3	
4	798.9	200.0	200	0	
5	999.0	200.1	200	0.1	
6	1199.1	200.1	200	0.1	
7	1399.4	200.3	200	0.3	
8	1599.6	200.2	200	0.2	
9	1799.4	199.8	200	−0.2	
10	1999.4	200.0	200	0	

Since the self-weight of each loading platform on the fore and back segment is 10 kg, when the measuring weights of 0 kg, 10 kg, 20 kg, 30 kg, 40 kg are respectively added on the loading platform, the equivalent load is respectively 20 kg, 40 kg, 60 kg, 80 kg, 100 kg, as shown in Fig. 22(b). In the course of the experiment, there is no slight slippage or lateral displacement found on the robot in the circumferential, radial and vertical direction. This phenomenon shows that the static rated load of the robot platform is not less than 100 kg. When the measuring weights of 40 kg are respectively added at A/B/C/D/E five different positions with a radial uniform spacing of 100 mm on the loading platform of the fore and back segment, the equivalent load is 100 kg respectively applied at these five different positions, as shown in Fig. 22(c). In the course of the experiment, there is also no slight slippage or lateral displacement found on the robot in the circumferential, radial and vertical direction. This phenomenon shows that the static offset rated load of the robot platform is also not less than 100 kg.

The time control precision and the spatial positioning accuracy of the creeping unit are closely related to the stability and reliability of the robot motion, so the test of these two accuracy indicators is critical. Tables 5 and 6 respectively show the maximum relative error of creeping period and the model positioning accuracy based on the mark point M of the principle prototype. During the 3 min motion test, the principle prototype carries the equivalent load of 100 kg with continuous movement of 10 creeping steps. The initial and end time point of each step are recorded in turn, and the actual creeping period of each step is calculated. By respectively comparing the actual values with the theoretical values, the absolute error of creeping period and the absolute motion error of the mark point M of each step are calculated, and then the relative error of creeping period of each step and the model positioning accuracy based on the mark point M can be got. From Table 5, it shows that the cumulative time error or time control precision of the creeping process is 0.01 s, which indicates that the creeping gait control has good timeliness. From Tables 5 and 6, it shows that the maximum relative error of creeping period is 0.28%, not exceeding the design index of 0.5%. Meanwhile, it also shows that the model positioning accuracy based on the mark point M is 0.6 mm, not exceeding the design index of 2 mm. And then, it can be obtained that the mean motion speed of the creeping unit is $(200 \times 10 - 0.6)\text{mm}/(18 \times 10 + 0.01)\text{s} \approx 11.107\ \text{mm/s} = 0.67\ \text{m/min}$, reaching the design index of 0.5m/min. It is proved that the developed wormlike creeping mobile robot has a certain dynamic carrying capacity and feasibility.

7. Conclusion and prospect

Aiming at developing a mobile robot platform to carry equipments or assist manipulator robots to complete the detection and maintenance tasks of the first wall in EAST nuclear fusion vessel, this paper focuses on the functional requirements and the design points, the system design scheme, the modular structure design and function analysis, the motion planning and control method of the robot platform. On the basis of these studies, a principle prototype is constructed, and the robot's function of steadily creeping on the imitative V-shaped circular slot at the bottom of the nuclear fusion vessel is achieved. In addition, the basic movement performance and bearing capacity of the principle prototype are tested, and the preliminary results are obtained.

The wormlike creeping mobile robot platform designed in this paper adopts chain structure, which is in series of n ($n \geq 2$) creeping units connected by telescopic elastic linkages. Each creeping unit is of three-part structure, which consists of a fore segment, a mid segment and a back segment connected by bidirectional universal joints. Based on this, a multifunctional chain platform with "$n \times 3$"type is formed, which has the advantages of simple reconfigurable structure, easy control method, low manufacturing cost, good operational stability and wide motion range within the entire bottom of the EAST nuclear fusion vessel.

Although achieving the creeping movement function in the EAST nuclear fusion vessel from the basic principle, the principle prototype developed in this paper still has some technical

defects and deficiencies, which are mainly reflected in the following aspects: the insufficient resistance to extreme physical environmental conditions, the lack of a certain force sensing feedback device, the inadequate dynamic traction and response characteristics, the inadequate degree of cooperation with other remote maintenance systems of the robot, and so on. In the future work, the present research results should be developed by optimizing the design scheme and improving the technical level, to promote the sustainable development of the automatic maintenance technology for the nuclear fusion experimental device.

Acknowledgments

This research work was funded by the National Natural Science Foundation of China (NSFC) under Grant No. 61503361 and supported by China Domestic Research Project for the International Thermonuclear Experimental Reactor (ITER) under Grant No. 2012GB102007. The authors wish to thank the research group for their great contributions to the present research. The views and opinions expressed in this paper are the sole responsibility of the authors.

References

[1] R. Pampin, A. Davis, J. Izquierdo, D. Leichtle, M.J. Loughlin, J. Sanz, et al., Developments and needs in nuclear analysis of fusion technology, Fusion Eng. Des. 88 (2013) 454–460.
[2] C. Damiani, C. Annino, S. Balagué, P. Bates, F. Ceccanti, T. Di Mascio, et al., The European contribution to the ITER remote maintenance, Fusion Eng. Des. 89 (2014) 2251–2256.
[3] Yuntao Song, Damao Yao, Songata Wu, Peide Weng, Structural analysis and manufacture for the vacuum vessel of experimental advanced superconducting tokamak (EAST) device, Fusion Eng. Des 81 (2006) 1117–1122.
[4] Shanshuang Shi, Yuntao Song, Yong Cheng, Eric Villedieu, Vincent Bruno, Hansheng Feng, et al., Conceptual design main progress of EAST articulated maintenance arm (EAMA) system, Fusion Eng. Des. 104 (2016) 40–45.
[5] Weijun Zhang, Zeyu Zhou, Jianjun Yuan, Liang Du, Ziming Mao, Analysis and optimization on in-vessel inspection robotic system for EAST, Fusion Eng. Des. 101 (2015) 192–196.
[6] B. Haist, S. Mills, A. Loving, Remote handling preparations for JET EP2 shutdown, Fusion Eng. Des. 84 (2009) 875–879.
[7] S. Sanders, A. Rolfe, The use of virtual reality for preparation and implementation of JET remote handling operations, Fusion Eng. Des. 69 (2003) 157–161.
[8] S. Kakudate, K. Shibanuma, Tail deployment and storage procedure and test for ITER blanket remote maintenance, Fusion Eng. Des. 65 (2003) 133–140.
[9] O. David, A.B. Loving, J.D. Palmer, et al., Operational experience feedback in JET remote handling, Fusion Eng. Des. 75 (2005) 519–523.
[10] Xuebing Peng, Jianjun Yuan, Weijun Zhang, Yang Yang, Yuntao Song, Kinematic and dynamic analysis of a serial-link robot for inspection process in EAST vacuum vessel, Fusion Eng. Des. 87 (2012) 905–909.
[11] X.B. Peng, Y.T. Song, C.C. Li, M.Z. Lei, G. Li, Conceptual design of EAST flexible in-vessel inspection system, Fusion Eng. Des. 85 (2010) 1362–1365.
[12] Gregory Dubus, Adrian Puiu, Philip Bates, Carlo Damiani, Roger Reichle, Jim Palmer, Progress in the design and R&D of the ITER in-vessel viewing and metrology system (IVVS), Fusion Eng. Des. 89 (2014) 2398–2403.
[13] Y.T. Song, X.B. Peng, H. Xie, X.F. Liu, L.M. Bao, Z.B. Zhou, et al., Plasma facing components of EAST, Fusion Eng. Des. 85 (2010) 2323–2327.
[14] Vo-Gia Loc, Se-goh Roh, Ig Mo Koo, Duc Trong Tran, Ho Moon Kim, Hyungpil Moon, et al., Sensing and gait planning of quadruped walking and climbing robot for traversing in complex environment, Robot. Auton. Syst. 58 (2010) 666–675.
[15] Taro Nakamura, Takashi Kato, Tomohide Iwanaga, Yoichi Muranaka, Peristaltic crawling robot based on the locomotion mechanism of earthworms, IFAC Proc. 39 (2006) 139–144.
[16] Jian-wei Zhao, Xiao-gang Ruan, Flexible two-wheeled self-Balancing mobile robot, IFAC Proc. 42 (2009) 117–124.
[17] J. Liu, B.-Y. Ma, N. Fry, A. Pickering, S. Whitehead, N. Somjit, et al., Exploration robots for harsh environments and safety, IFAC-PapersOnLine 48 (10) (2015) 41–45.
[18] P. Long, S. Liu, Y. Wu, F.D.S. the Team, Design and testing of the fusion virtual assembly system FVAS 1.0, Fusion Eng. Des. 82 (2007) 2062–2066.
[19] Maoxun Li, Shuxiang Guo, Hideyuki Hirata, Hidenori Ishihara, Design and performance evaluation of an amphibious spherical robot, Robot. Auton. Syst. 64 (2015) 21–34.